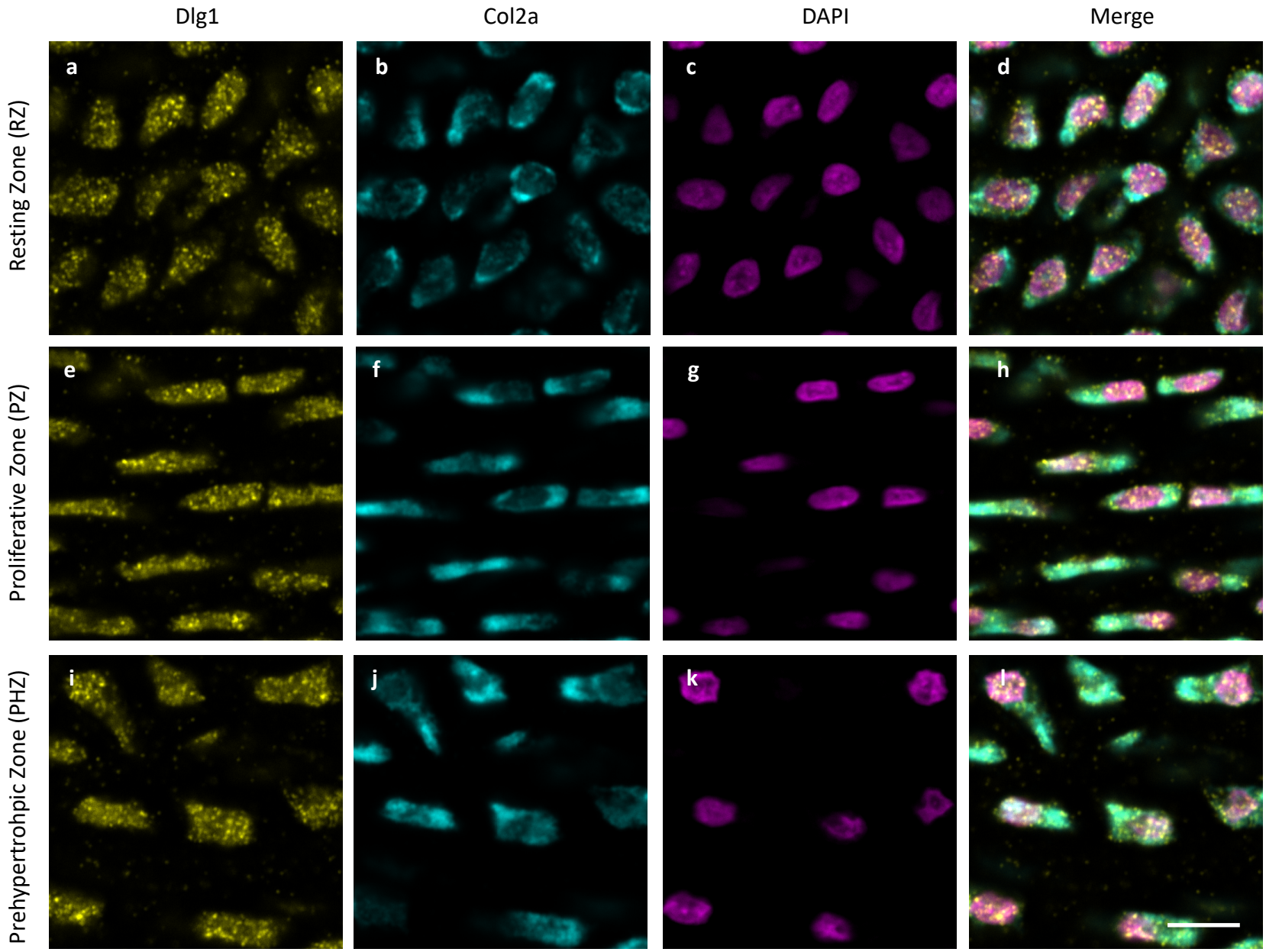
Dlg1
Col2a
DAPI
Merge
Resting Zone (RZ)
Proliferative Zone (PZ)
Prehypertrohpic Zone (PHZ)
a
b
c
d
e
f
g
h
i
j
k
l

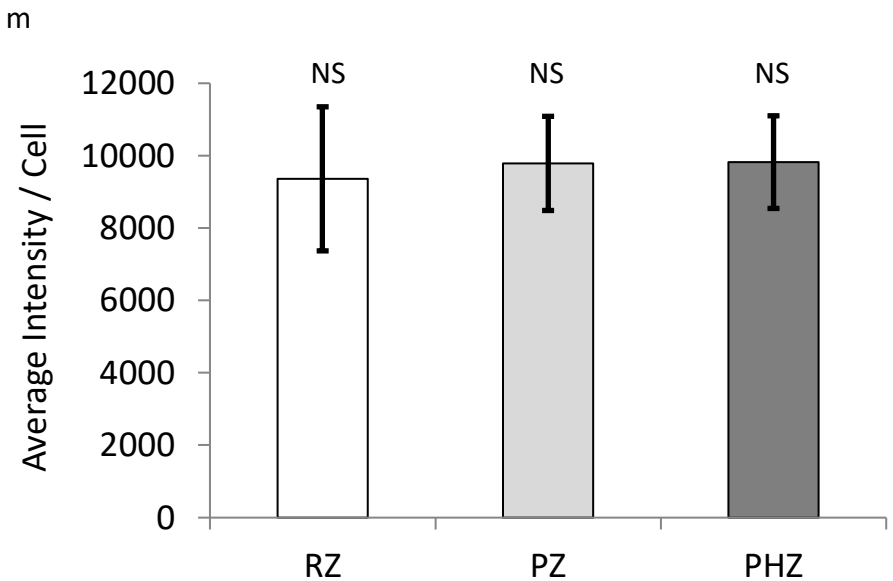
m
Average Intensity / Cell
12000
10000
8000
6000
4000
2000
0
NS
NS
NS
RZ
PZ
PHZ

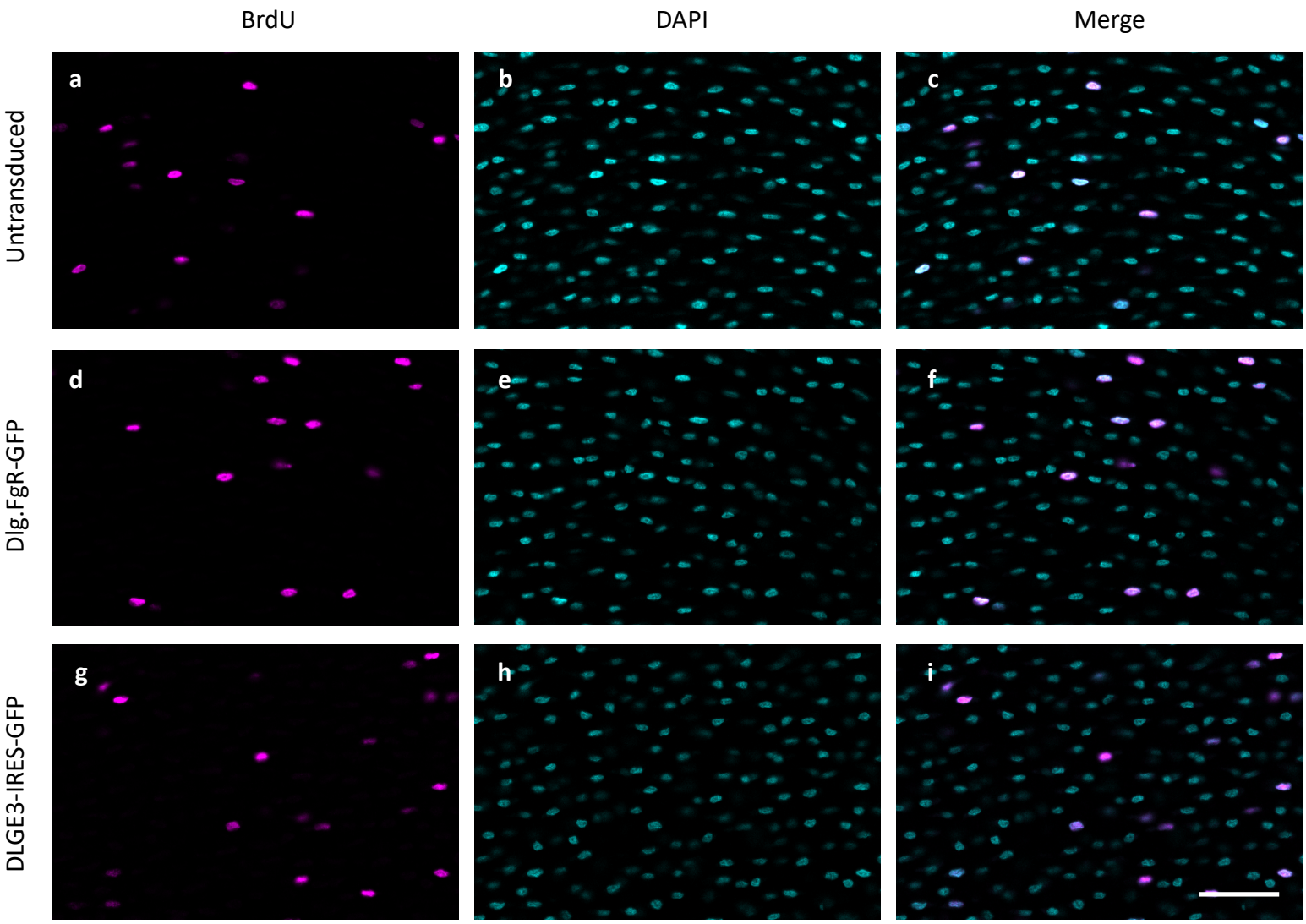
BrdU
DAPI
Merge
Untransduced
Dlg.FgR-GFP
DLGE3-IRES-GFP
a
b
c
d
e
f
g
h
i

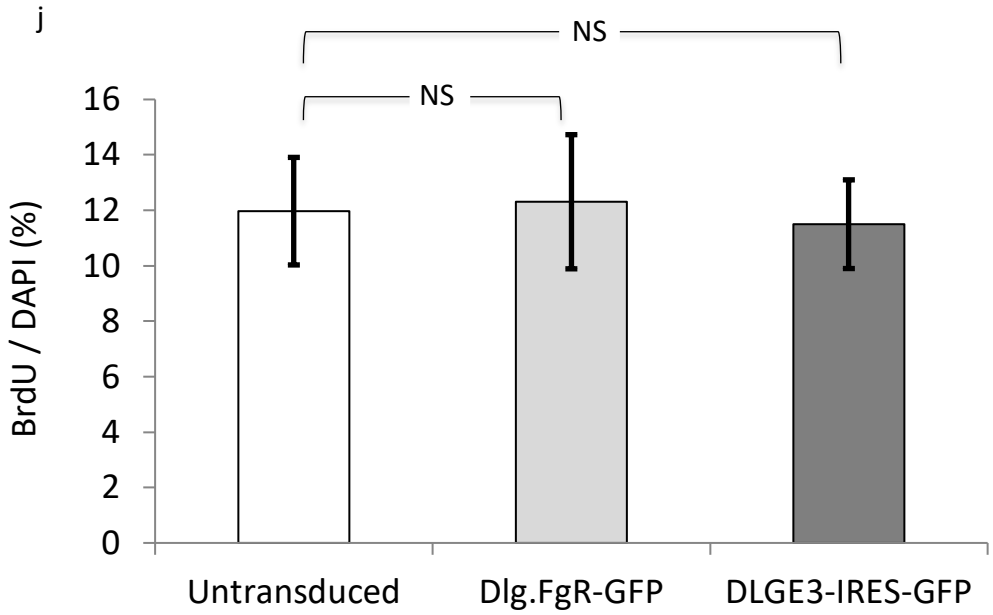
j
NS
NS
BrdU / DAPI (%)
16
14
12
10
8
6
4
2
0
Untransduced
Dlg.FgR-GFP
DLGE3-IRES-GFP

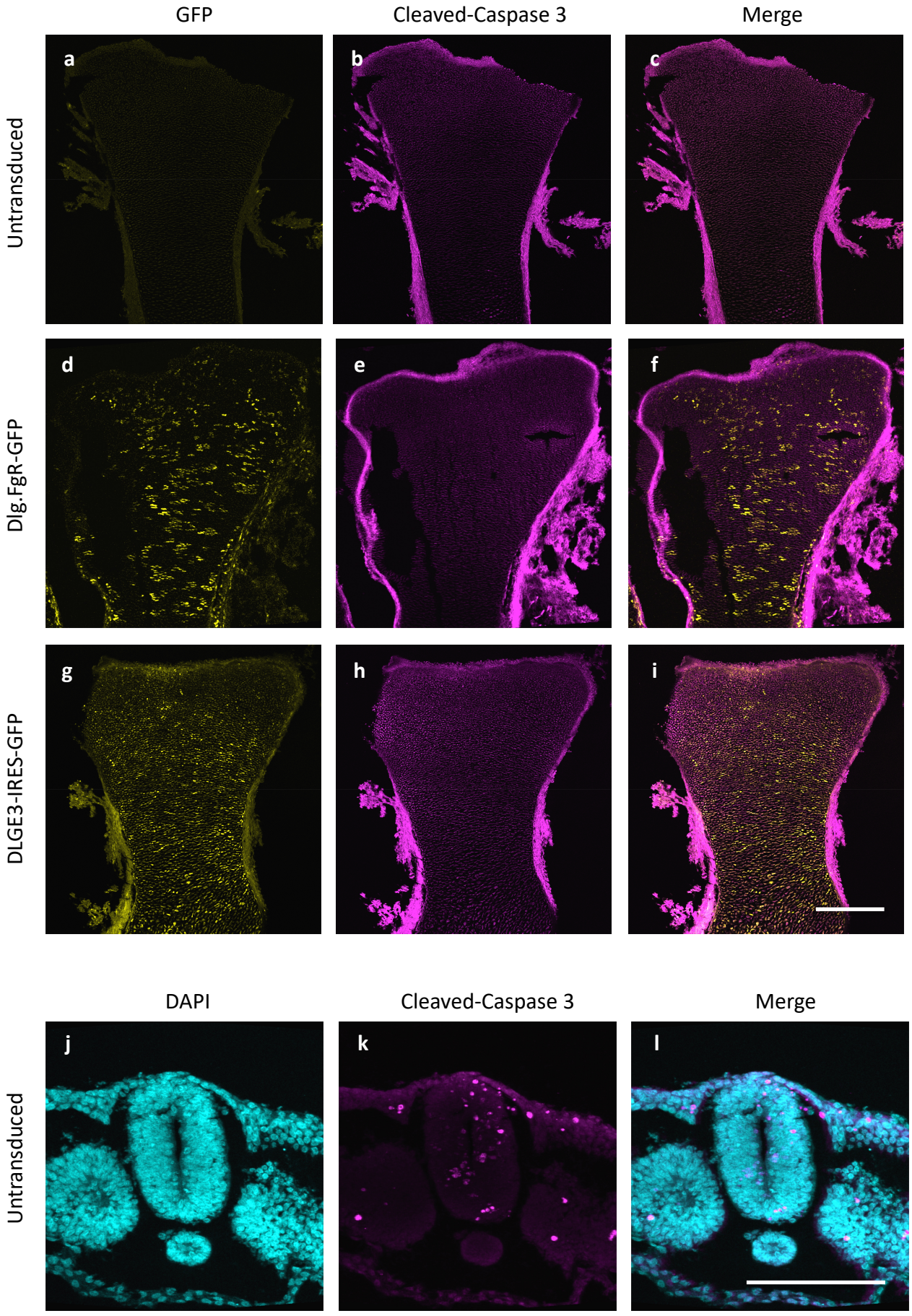
GFP
Cleaved-Caspase 3
Merge
Untransduced
Dlg.FgR-GFP
DLGE3-IRES-GFP
a
b
c
d
e
f
g
h
i
DAPI
Cleaved-Caspase 3
Merge
Untransduced
j
k
l

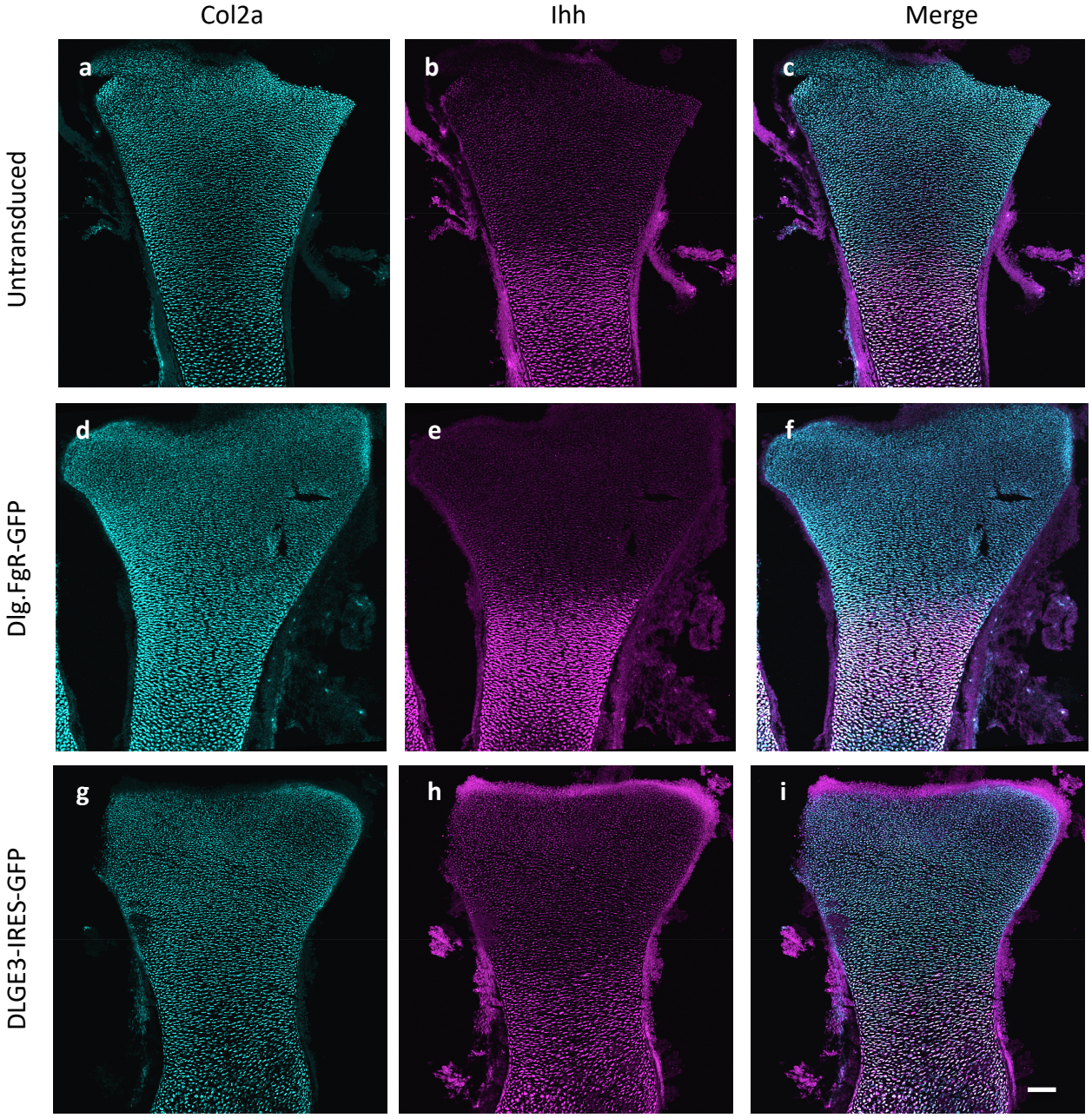

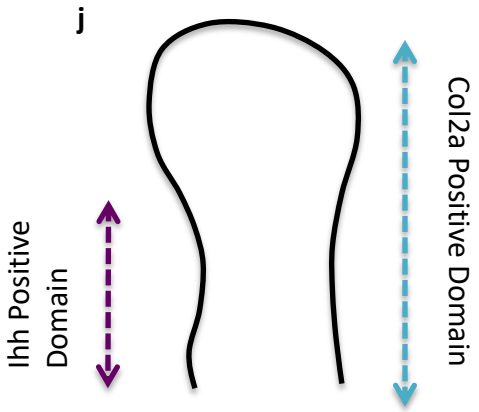

Fractional Length =

$$\frac{\text{Length of Ihh Positive Domain}}{\text{Length of Col2a Positive Domain}}$$

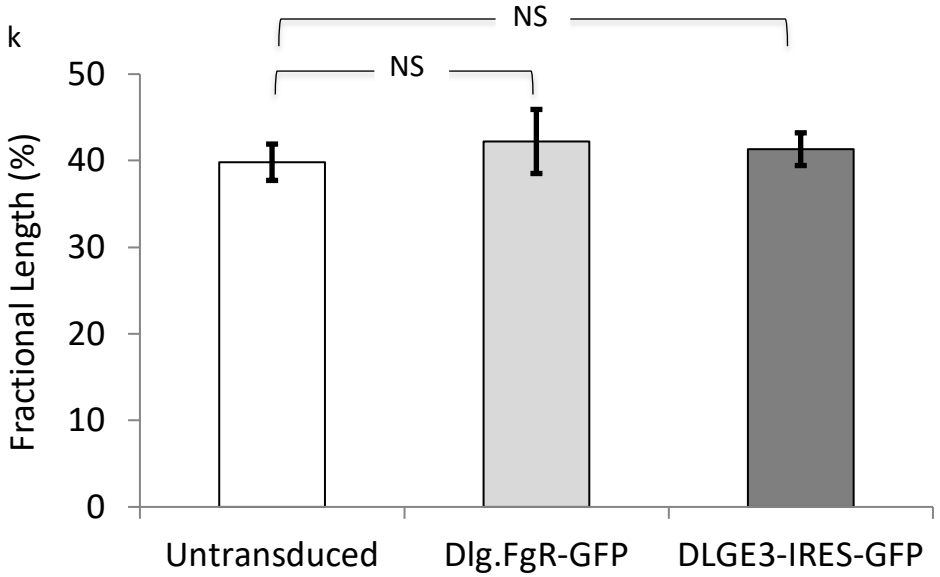

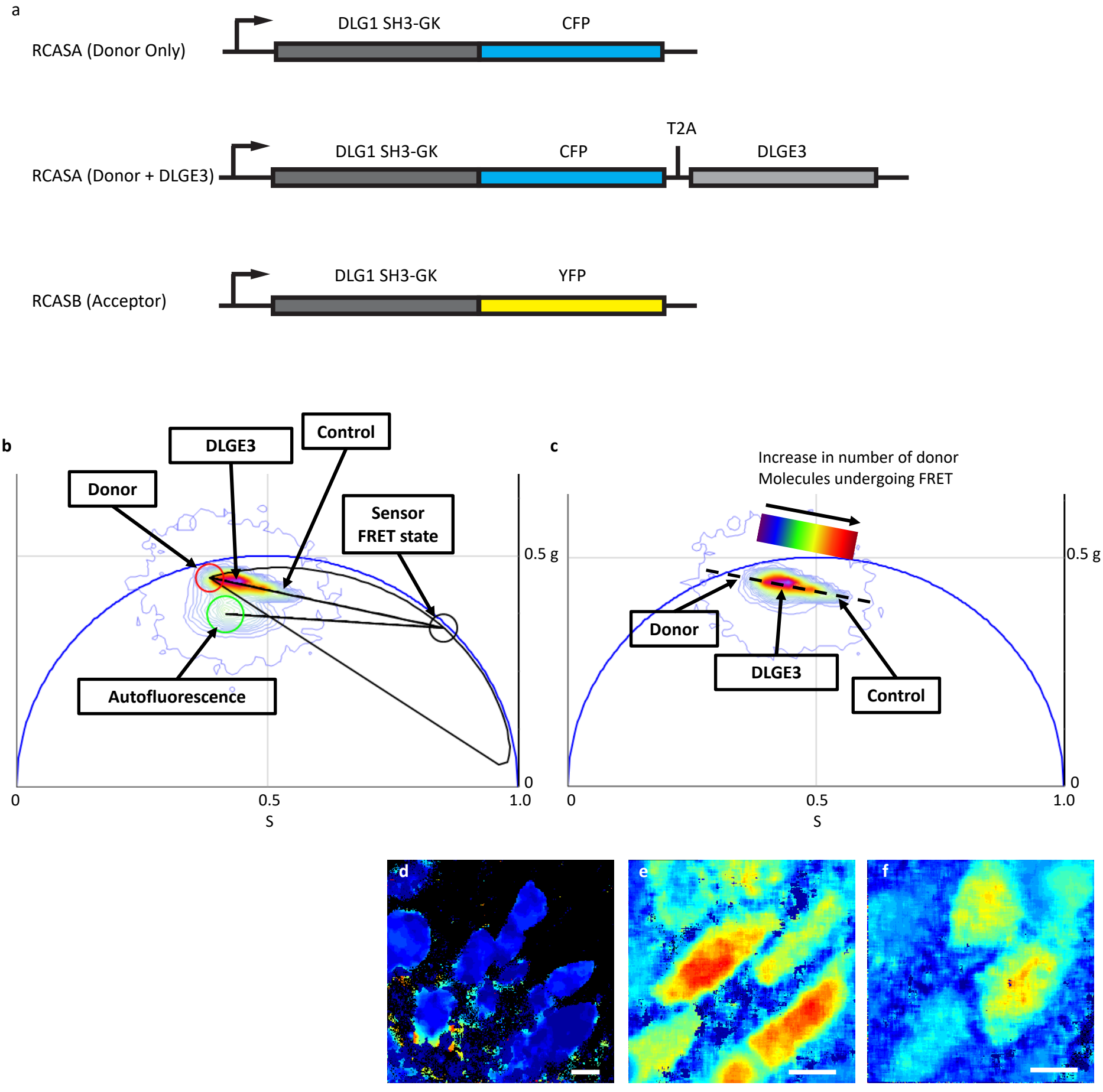
a
RCASA (Donor Only)
DLG1 SH3-GK
CFP
RCASA (Donor + DLGE3)
T2A
DLG1 SH3-GK
CFP
DLGE3
RCASB (Acceptor)
DLG1 SH3-GK
YFP
b
DLGE3
Control
Donor
Sensor
FRET state
Autofluorescence
0.5 g
0
0
0.5
1.0
S
c
Increase in number of donor
Molecules undergoing FRET
0.5 g
Donor
DLGE3
Control
0
0
0.5
1.0
S
d
e
f

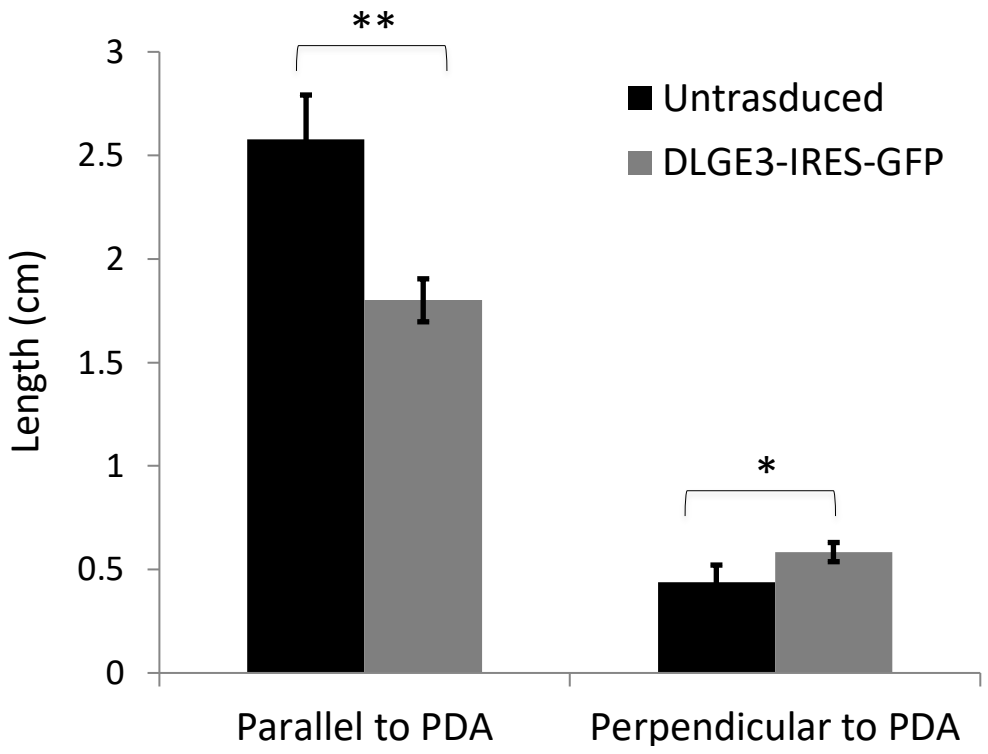
**
*
3
2.5
2
1.5
1
0.5
0
Length (cm)
Untrasduced
DLGE3-IRES-GFP
Parallel to PDA
Perpendicular to PDA

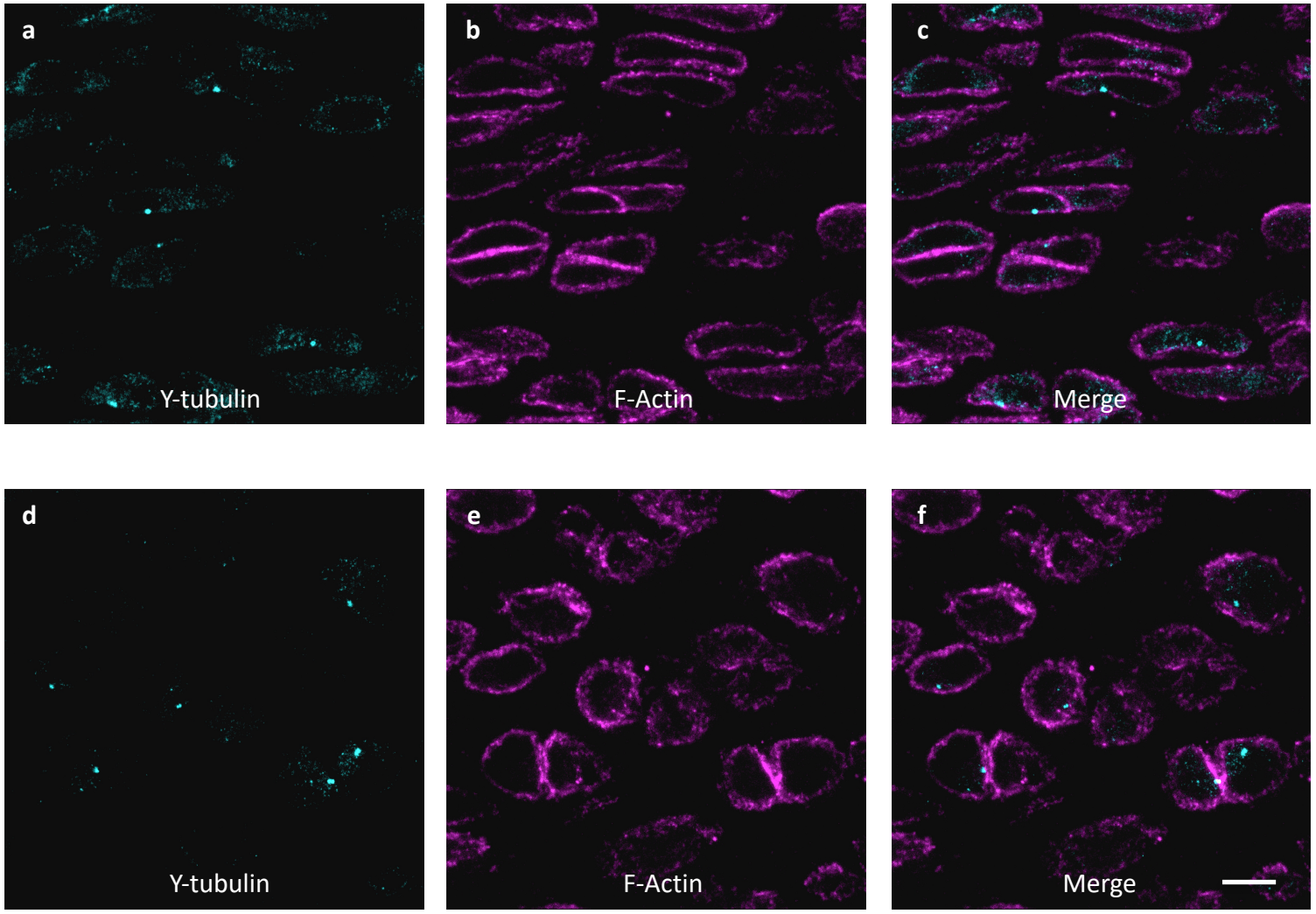
a
b
c
Dlg1 +/+
Y-tubulin
F-Actin
Merge
d
e
f
Dlg1 -/-
Y-tubulin
F-Actin
Merge

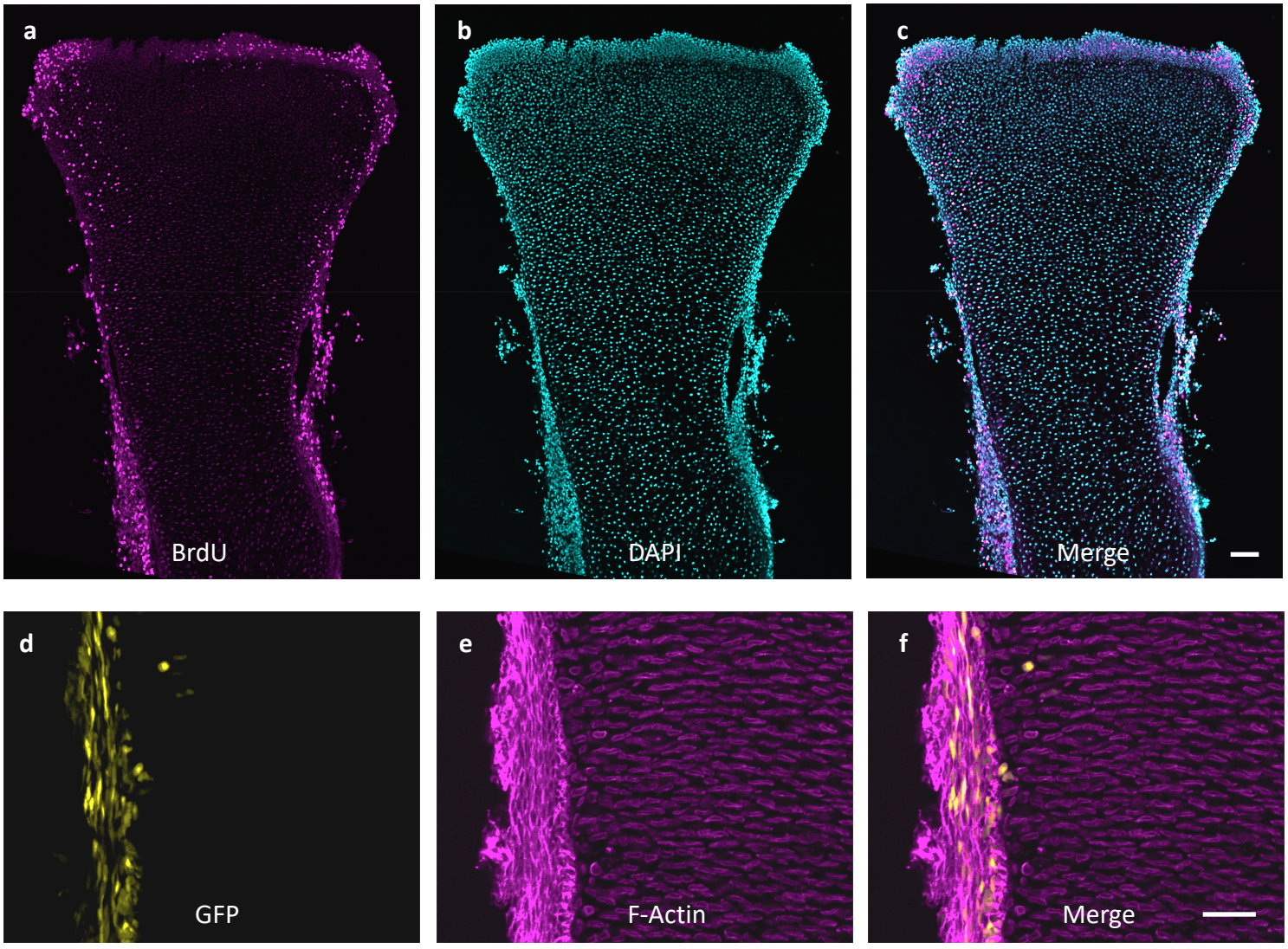
a
BrdU
b
DAPI
c
Merge
d
GFP
e
F-Actin
f
Merge

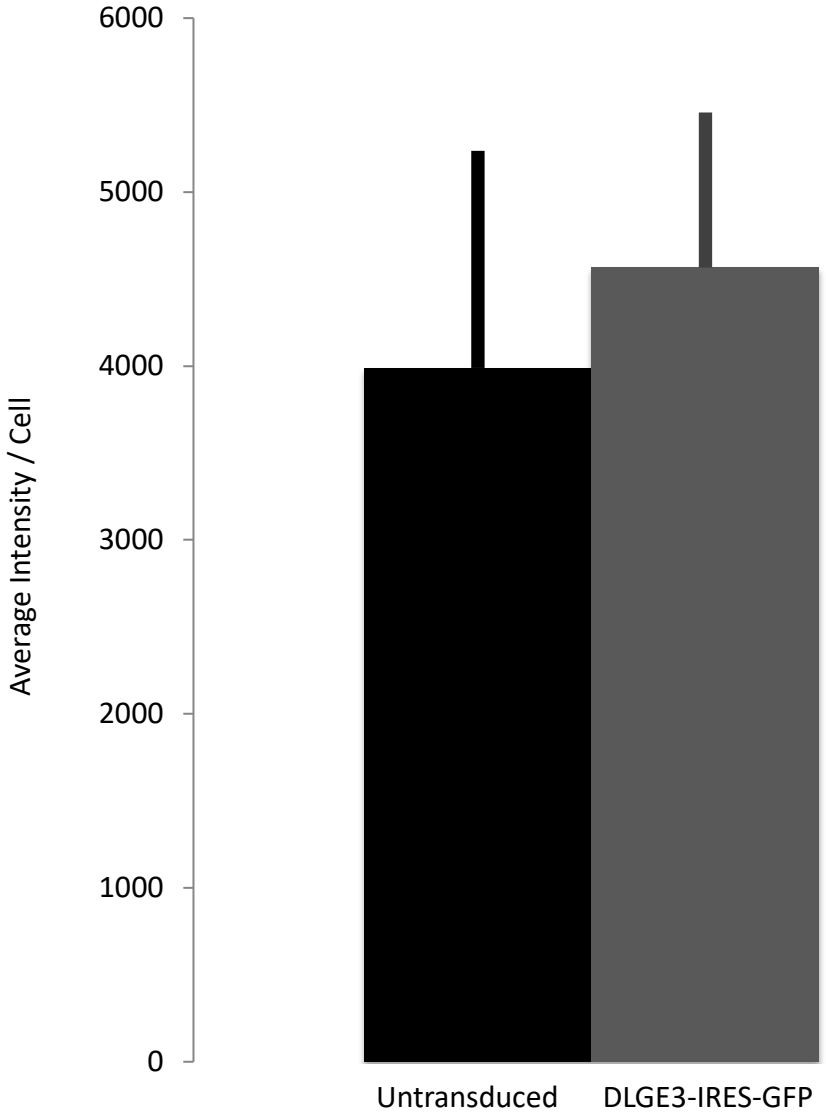
6000
5000
4000
3000
2000
1000
0
Average Intensity / Cell
Untransduced
DLGE3-IRES-GFP

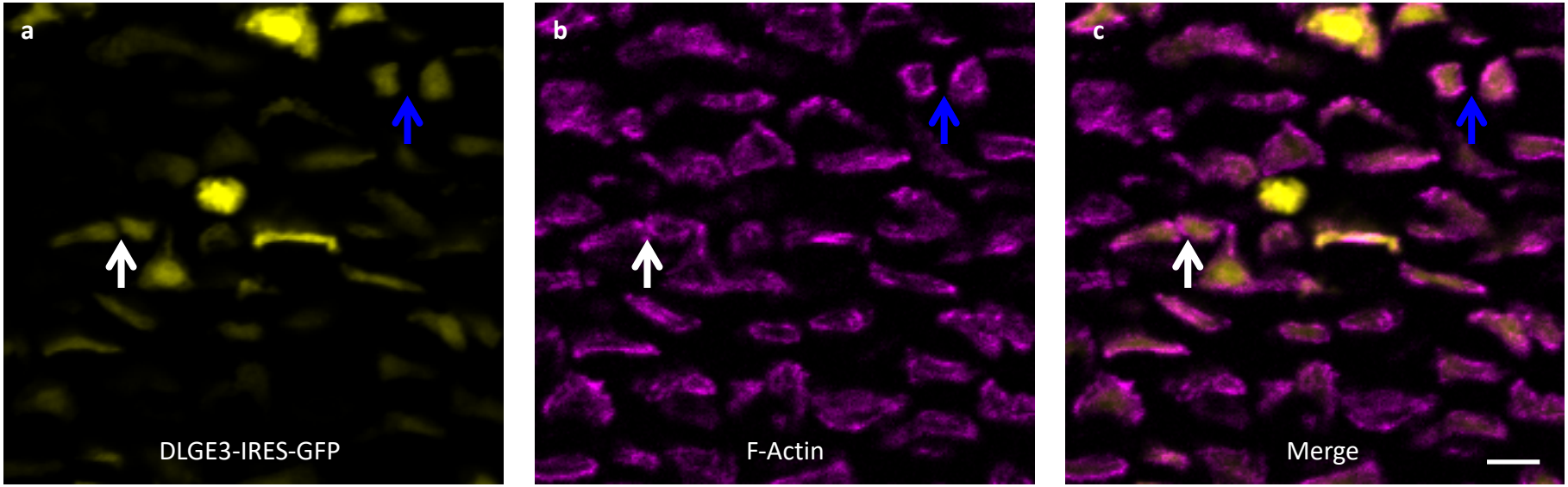
a
DLGE3-IRES-GFP
b
F-Actin
c
Merge

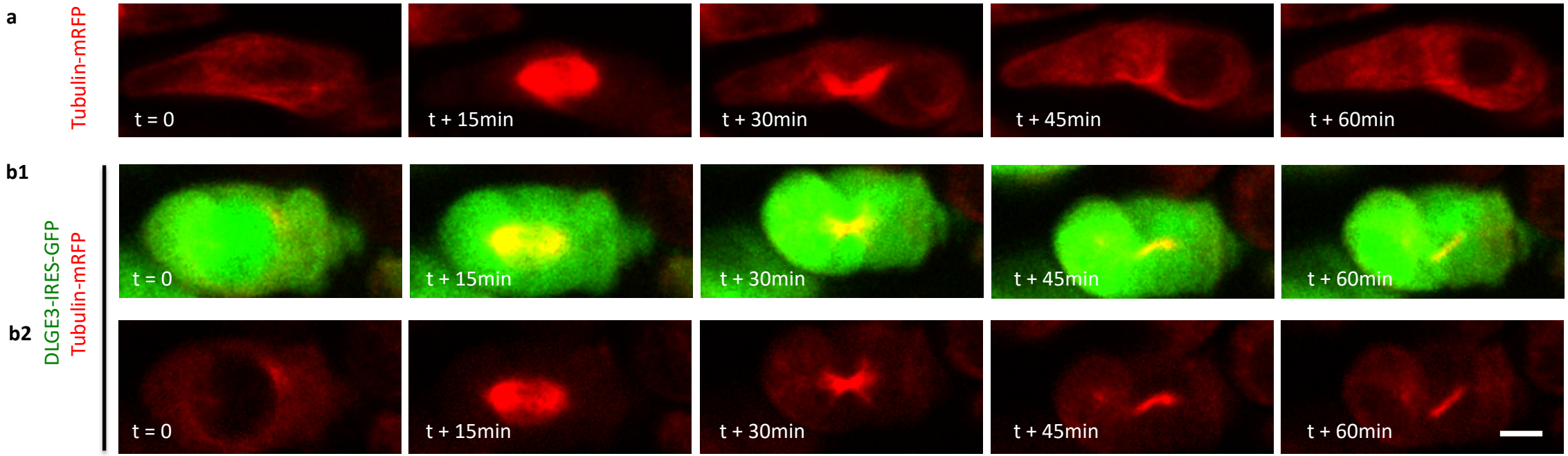
a
Tubulin-mRFP
t = 0
t + 15min
t + 30min
t + 45min
t + 60min
b1
DLGE3-IRES-GFP
Tubulin-mRFP
t = 0
t + 15min
t + 30min
t + 45min
t + 60min
b2
t = 0
t + 15min
t + 30min
t + 45min
t + 60min

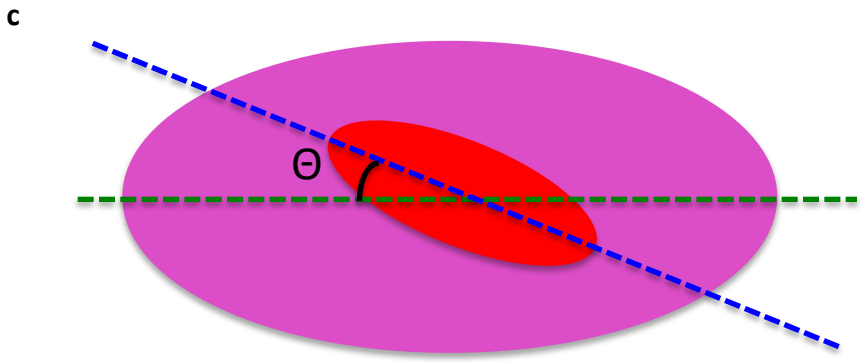
c
Θ

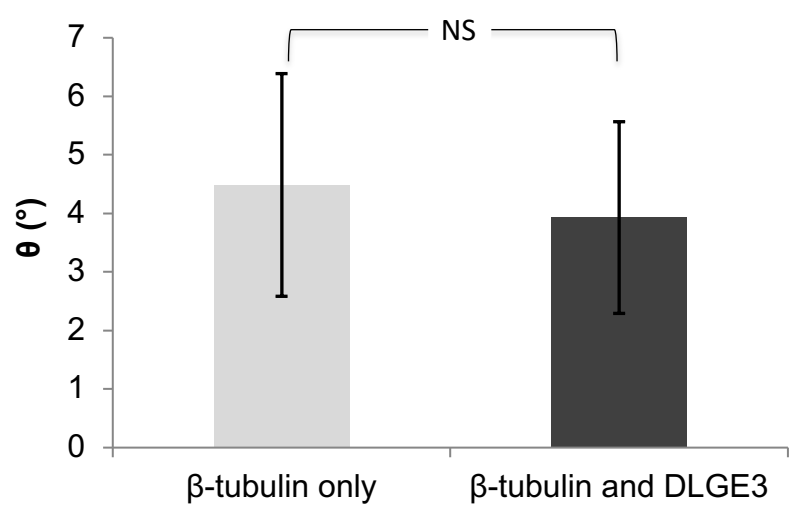
d
NS
θ (°)
0
1
2
3
4
5
6
7
β-tubulin only
β-tubulin and DLGE3

IP Ab: mouse anti-pan-MAGUK
Blot primary Ab: mouse anti-Beta-catenin
Blot secondary Ab: goat anti-mouse IgG (H+L) Alexa780
1: chondrocyte lysate
2: IP from lysate
Arrow: Beta-catenin
Arrowhead: mouse IgG (H+L chains)

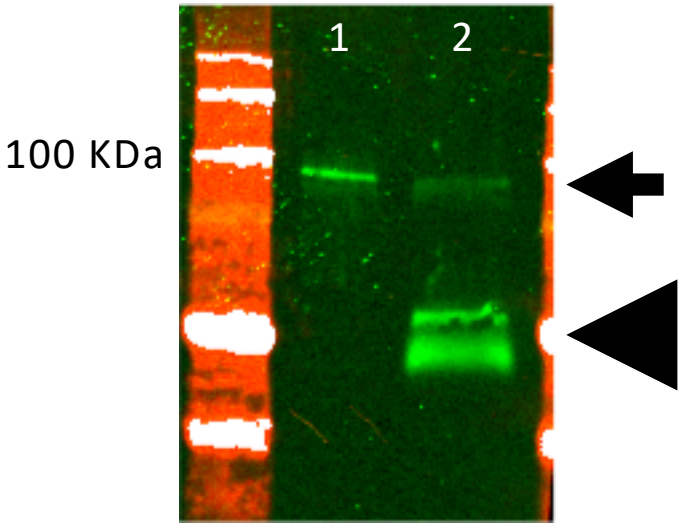

Supplemental Table S1. Mass spectroscopic analysis of E13.5 chicken humerus cartilage. Proteins ~80-125 kDa were identified from SDS-page gel electrophoresis samples. Dlg1 was moved to the top of this partial list to highlight its presence in the analysis and is the only MAGUK identified. A comprehensive list from this analysis will be made available.

Fasta headers	Mol. Wt. [kDa]	Score	Intensity	iBAQ	Protein IDs
Discs large MAGUK scaffold protein 1	97.307	1.7324	2467300	68535	A0A1D5P102
Endoplasmin	91.213	214.99	3050400000	78214000	A0A1L1S093
Nucleolin	75.399	17.71	839190000	27071000	A0A1D5NZ30
Heat shock cognate protein HSP 90-beta	80.018	62.096	553000000	16265000	A0A1D5PHC5
Valosin containing protein	89.324	36.374	635690000	14127000	Q5ZMU9
Gelsolin	85.831	27.765	361720000	10639000	O93510
Procollagen-lysine,2-oxoglutarate 5-dioxygenase 2	87.01	46.35	338700000	7876700	F1NXB0
Interleukin enhancer binding factor 3	66.548	34.155	197030000	6356000	A0A1D5PR95
Alpha-actinin-4	91.294	30.619	295330000	6027200	A0A1D5P522;
Heterogeneous nuclear ribonucleoprotein U	91.61	56.076	207830000	5937900	F1NSP8
Decorin	39.686	17.778	111390000	5862700	P28675
Histone H1.01	22.044	17.992	38079000	5439800	P08284
Karyopherin subunit beta 1	119.94	2.1553	267130000	5137100	A0A1D5P1W7
MICOS complex subunit MIC60	79.223	55.089	196130000	4669800	F1P3U1
Prolyl 3-hydroxylase 1	81.675	8.4901	155860000	4584300	Q6JHU8
Aconitate hydratase, mitochondrial	84.678	7.1322	148440000	4366000	A0A1D5PZ66
Alpha-actinin-1	102.43	29.224	229010000	4240900	A0A1D5P9P3
Cell cycle associated protein 1	77.987	15.544	88603000	4219200	Q5XNV3
Lysosome-associated membrane glycoprotein 1	10.132	4.6538	13536000	3384000	A0A1L1S0W8
Splicing factor 3a subunit 1	88.486	67.007	133530000	3256800	F1NU16
26S proteasome non-ATPase regulatory subunit 1	106.06	12.267	145340000	3092400	Q5F418
Far upstream element-binding protein 2	80.643	33.489	128910000	3069400	Q8UVD9
DNA topoisomerase 1	89.693	37.893	114840000	3022100	R4GM79
Catenin alpha 1	100.04	24.757	138950000	2956400	A0A1D5P7X0
Integrin beta	88.399	15.851	106430000	2956300	A0A1D5PNB4
Aspartate beta-hydroxylase	80.122	7.0537	92353000	2886000	A0A1D5PAN4
Adseverin	78.852	23.396	110590000	2835600	A0A1D5PBC3
Programmed cell death 6 interacting protein	97.314	11.72	132960000	2770100	Q5ZJ70
Cold shock domain-containing protein E1	88.631	41.571	119940000	2725900	E1BQF9
Eukaryotic translation initiation factor 3 subunit B	85.318	3.2831	97679000	2713300	A0A1D5PTG6
Dynamin 1	97.234	20.281	116480000	2377000	E1BXY4

sup movie 1 images.pdf

753 x 185

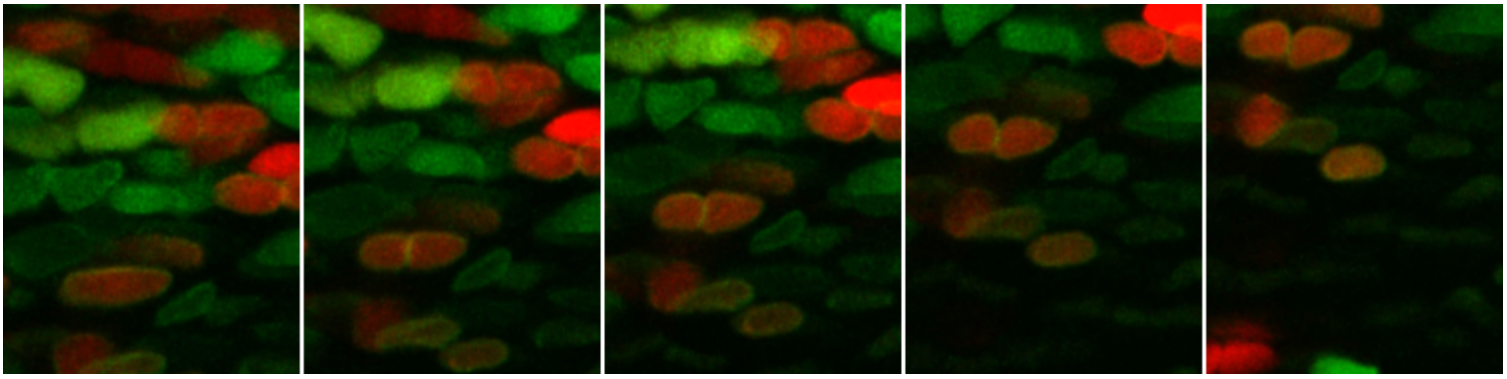

sup movie 2 images.pdf

646 x 322

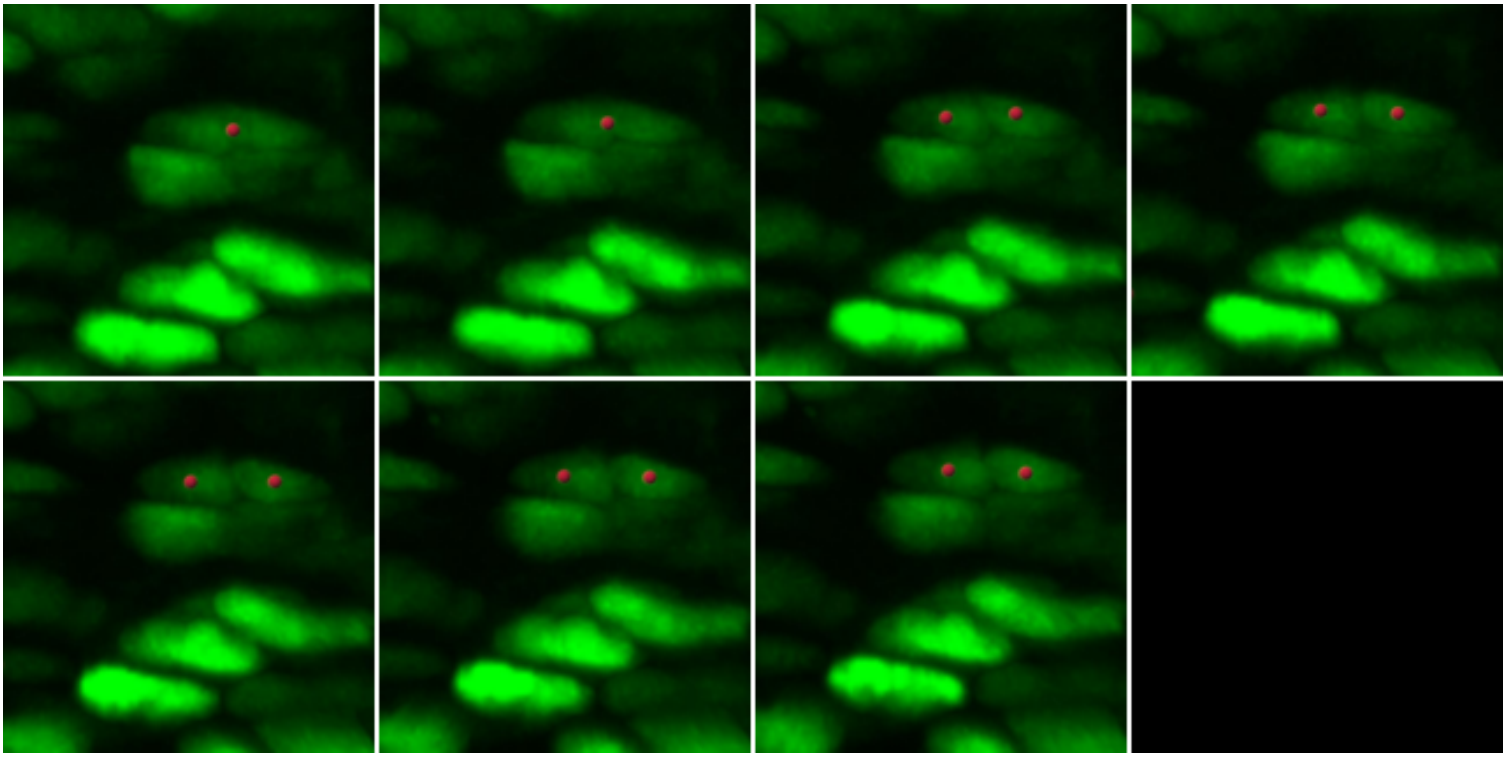

sup movie 3 images.pdf

646 x 322

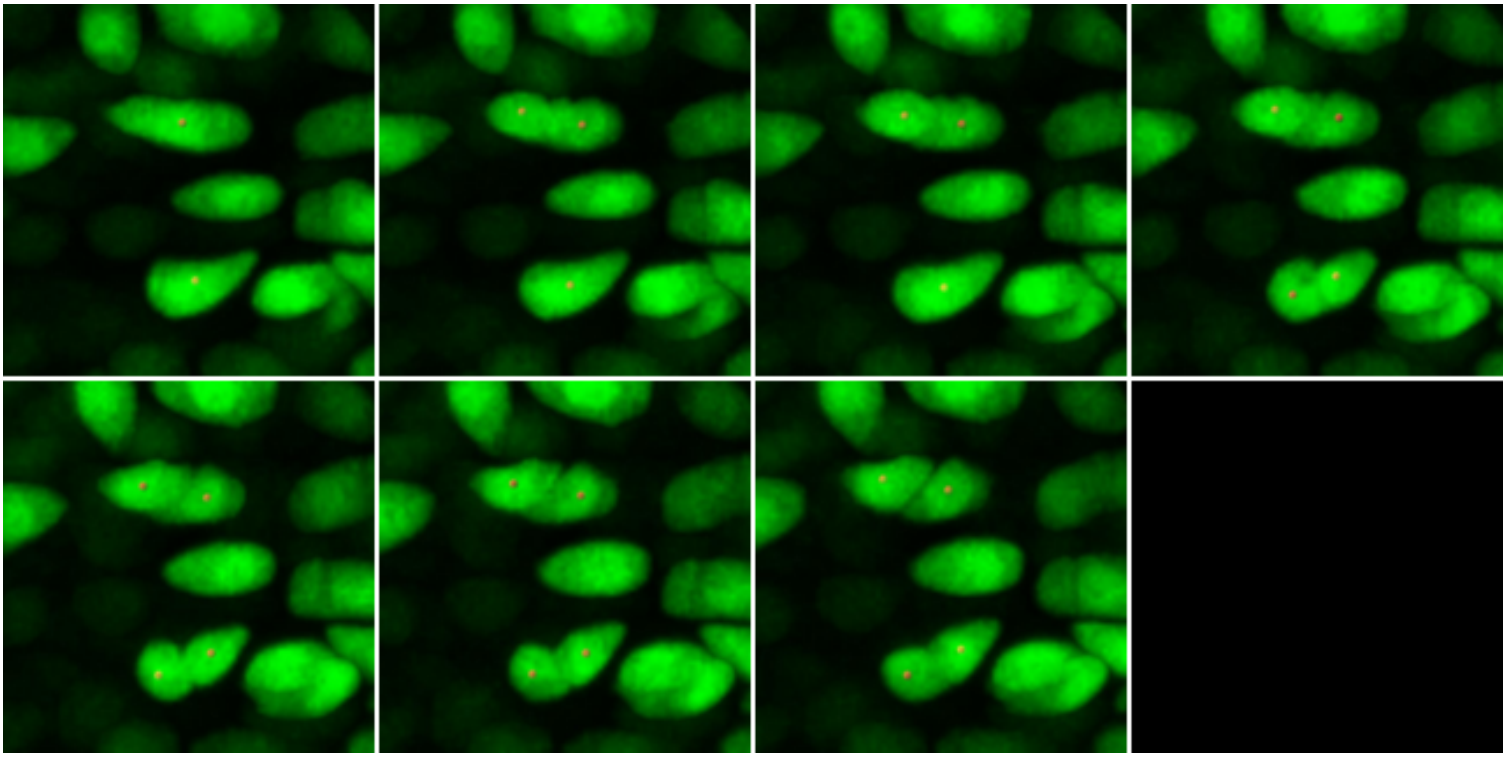

Supplemental Figure 1. Dlg1 mRNA is expressed in distinct zones of cartilage

High magnification images of chick humeri hybridized with anti-Dlg1 probes (a, e, i), anti-Col2a probes (b, f, j, marker of chondrocytes) and stained with DAPI (c, g, k). Dlg1 mRNA is expressed in both nucleus and cytoplasm (a-l). Fluorescent quantification of Dlg1 mRNA showed that it is uniformly expressed in the resting (RZ), proliferative (PZ) and prehypertrophic zones (PHZ) (m). N = 5 humeri. NS denotes no significant difference (T-test). Scale bar: 15 μm.

Supplemental Table S1. Mass spectroscopic analysis of E13.5 chicken humerus cartilage. Proteins ~80-125 kDa were identified from SDS-page gel electrophoresis samples. Dlg1 was moved to the top of this partial list to highlight its presence in the analysis and is the only MAGUK identified. A comprehensive list from this analysis will be made available.

Supplemental Figure 2. Exogenous Dlg.FingR and DLGE3 do not affect normal mitotic cell division in the proliferative zone of cartilage

BrdU and DAPI staining was performed on untransduced chicken humeri (a-c), humeri expressing Dlg.FingR-GFP (d-f) and humeri expressing DLGE3-IRES-GFP (g-i). The similar ratio between BrdU and DAPI positive cells in different conditions (j) suggests mitotic cell division was not significantly impacted by the expression of Dlg.FingR or DLGE3. N = 5 untransduced, 5 Dlg.FingR-GFP expressing and 5 DLGE3-IRES-GFP expressing humeri. NS denotes no significant difference (T-test). Scale bar: 70 μm.

Supplemental Figure 3. Exogenous Dlg.FingR and DLGE3 do not cause apoptosis in cartilage

Untransduced chicken humeri (a-c), humeri expressing Dlg.FingR-GFP (d-f) and humeri expressing DLGE3-IRES-GFP (g-i) did not contain any apoptotic chondrocytes, as demonstrated by

immunofluorescence using anti-cleaved-caspase 3 antibody (b, e, h). As a positive control, this antibody detected apoptotic cells inside chicken neural tube and somite (j-l). N = 5 untransduced, 5 Dlg.FingR-GFP expressing and 5 DLGE3-IRES-GFP expressing humeri. Scale bars: 150 μm.

Supplemental Figure 4. Exogenous Dlg.FingR and DLGE3 do not affect normal chondrocyte differentiation in cartilage

HCR was performed on the adjacent tissues sections used in Supplemental figure 3; these samples include untransduced chicken humeri (a-c), humeri expressing Dlg.FingR-GFP (d-f) and humeri expressing DLGE3-IRES-GFP (g-i). Col2a (a, d, g) and Ihh (b, e, h) was the marker for all chondrocytes and prehypertrophic chondrocytes, respectively. Cell differentiation rate was determined by the fractional length between Ihh and Col2a positive domains (j). The similar fractional length in different conditions (k) show Dlg.FingR-GFP and DLGE3-IRES-GFP do not affect normal cell differentiation. N = 5 untransduced, 5 Dlg.FingR-GFP expressing and 5 DLGE3-IRES-GFP expressing humeri. NS denotes no significant difference (T-test). Scale bars 150 μm.

Supplemental Figure 5. FLIM-FRET showing DLGE3 prevents Dlg1 multimerization in cartilage

(a) Construction of retroviral vector harboring Dlg1 FRET sensor. Donor with or without DLGE3 was subcloned into RCAS virus coated with envelope type-A protein. Acceptor was subcloned into the virus coated with envelope type-B protein. Coinfection of both viruses permitted donor and acceptor to be expressed within the same chondrocytes. In some cases, cells were transduced by one virus, which were used as internal controls. The transduced chicken metacarpals were explanted for FLIM-FRET analysis. (b-d) Phasor plot of fluorescence lifetime (b) and sensor populations undergoing FRET (c) in multiple chondrocytes showed similar but more dramatic distribution patterns to the phasor analysis of portions of

chondrocytes in Fig. 3d-i. This phasor includes measurements from chondrocytes expressing donor only (d), FRET sensor without (e) and with DLGE3 (f). Scale bars = 5 μm.

Supplemental Figure 6. Dlg1 is required for normal dimensions of cartilage

Compared with untransduced chicken cartilage, the ones expressing DLGE3 is shorter (parallel to PDA) and wider (perpendicular to PDA). ** denotes significant difference (T-test). N is 10 and 8 for untransduced and DLGE3 expressing tissues, respectively.

Supplemental Figure 7. Dlg1 is required for normal chondrocyte cell polarity in mouse

Similar analysis of MTOCs orientation in chick (Figure 5a-i) was performed in mice humerus. In wild-type mice, MTOCs were distributed on the longitudinal sides of cells (a-c). In contrast, MTOCs was misoriented in *Dlg1*$^{-/-}$ mice (d-f). N = 3 wild-type and 5 Dlg$^{-/-}$ humeri Scale bar: 10 μm.

Supplemental Figure 8. Dlg1's function in the perichondrium/periosteum is not required for chondrocyte cell polarity

To determine whether chondrocyte cell polarity is affected by Dlg1's function in neighboring tissue, mosaic analysis in chicken was performed. During infection, RCAS RNA can only enter host nuclei during mitosis when nucleus membrane is broken. Hence, the more active cell division, the more likely viral RNA integrates into host chromosomes. As shown by short-pulse (2 hours) BrdU labeling in chicken cartilage, whereas many perichondrium/periosteum cells incorporated BrdU, chondrocytes did not (a-c), a sign that perichondrium/periosteum cells divide faster than chondrocytes. As a result, the very low titer virus (1 x 10^7) expressing RCAS-DLGE3-IRES-GFP did not transduce chondrocytes, but still transduce

the perichondrium/periosteum (d). Normalization to phalloidin signal revealed normal chondrocyte cell morphologies within these mosaic limbs (e). N = 4 transduced humeri. Scale bar: 35 μm.

Supplemental Figure 9. Immunostaining reveals DLGE3 does not significantly reduce Dlg1 protein

(a) Densitometric analysis of Dlg1 immunostaining shows there is no significant difference in Dlg1 abundance between those chondrocytes expressing DLGE3 (4566 ± 892 i.u./cell) and the untransduced control cells (3989 ± 1248 i.u./cell). N = 60 cells quantified per condition, 20 cells from 3 staining experiments.

Supplemental Figure 10. Chondrocytes expressing DLGE3 display oriented division but generate daughter cells with abnormal morphology

Chicken cartilage expressing DLGE3-IRES-GFP (a) was stained with phalloidin (b). A transduced mitotic cell had a normal contractile ring at the midbody and normal division orientation (white arrows). However, two transduced and separated daughter cells, inferred based on their relative positions, became abnormally shaped (blue arrows). Scale bar: 10 μm. N = 4 transduced chick humeri.

Supplemental Figure 11. Mitotic spindle is oriented along the elongation axes of mother cells during cell division

(a-b) Time-lapse images representative of mitosing cells expressing β-tubulin-mRFP only (a) and the ones coexpressing DLGE3-IRES-GFP (b). The same cell was presented in the combined channels (b1) and in red channel only (b2) to show co-expression of DLGE3 (green) and spindle microtubules (red), respectively. In both a and b, during cell division, mitotic spindle appears to be parallel to the elongation axes of the mother cells (t + 15mim). When the daughter cells were generated (t + 30min and afterwards), microtubules still maintained initial orientation in β-tubulin only expressing cells, but they appeared to be shifted in DLGE3 co-expressing cells. Scale bars: 3 μm.

(c) Diagram showing the approach to measure spindle orientation during cell division (t = 15min in a and b). A straight line (dashed blue) was drawn to connect the two pointed ends of the elliptical shaped network formed by spindle microtubules (red). The angle (θ) between the dashed blue line and the long axis (green dashed line) of the mother cell (purple) was calculated.

(d) Statistical analysis demonstrated that spindle orientation during cell division is below 5 degree in the cells only expressing β-tubulin (a) (n = 16) and the ones coexpressing DLGE3 (b) (n = 14), confirming that chondrocytes divide along cell elongation axis and that Dlg1 is not required for cell division orientation. NS denotes no significant difference (T-test).

Supplemental Figure 12. β-catenin co-immunoprecipitates with Dlg1 in chicken chondrocytes

To determine the biochemical association between Dlg1 and β-catenin in chondrocytes, co-immunoprecipitation was performed on chicken humeri. Tissues at E8 were lysed and exposed to the anti-pan-MAGUK antibody. The resulting precipitates were run on a SDS-PAGE gel, blotted, and probed with anti-β-catenin antibody. Lane 1 and 2 are whole lysates and IP lysates, respectively. This result is consistent with the previous finding of the interaction between Dlg1 and β-catenin (48). N = 7 chick humeri.

Supplementary Movie 1

Transverse view of chicken metacarpal expressing Dlg.FingR-GFP (green) and mCherry (red). Pseudocolored snapshots of the dividing cell were presented in Figure 2h. Scale bar: 5 μm.

Supplementary Movie 2

Transverse view of chicken metacarpal expressing GFP. Snapshots of the dividing cell were presented in Figure 6a. Scale bar: 5 μm.

Supplementary Movie 3

Transverse view of chicken metacarpal expressing DLGE3-IRES-GFP. Snapshots of the dividing cells were presented in Figure 6b and c. Scale bar: 5 μm.

Supplementary Movie 4

Transverse view of chicken metacarpal expressing β-tubulin-mRFP. Snapshots of the dividing cell were presented in Supplemental Figure 11a. Scale bar: 5 μm.

Supplementary Movie 5

Transverse view of chicken metacarpal expressing β-tubulin-mRFP (red) and DLGE3-IRES-GFP (gree). Snapshots of the dividing cell were presented in Supplemental Figure 11b1. Scale bar: 5 μm.

Supplementary Movie 6

The same move to Supplementary Movie 5 with only red channel presented to clearly show the orientation of mitotic spindle. Snapshots of the dividing cell were presented in Supplemental Figure 11b2. Scale bar: 5 μm.

Supplemental Data References

1. Arnesano, C. Santoro, Y. Gratton, E. Digital parallel frequency-domain spectroscopy for tissue imaging. *J Biomed Opt* **17**, 96014-1 (2012).

2. Stringari, C. Cinquin, A. Cinquin, O. Digman, M. Donovan, PJ. Gratton, E. Phasor approach to fluorescence lifetime microscopy distinguishes different metabolic states of germ cells in a live tissue. *Proc Natl Acad Sci USA* **108**, 13582 –13587 (2011).

3. Digman, MA. Caiolfa, VR. Zamai ,M. Gratton, E. The phasor approach to fluorescence lifetime imaging analysis. *Biophys J* **94**, L14–6 (2008).

4. Hinde, E. Digman, MA. Welch, C. Hahn, KM. Gratton, E. Biosensor förster resonance energy transfer detection by the phasor approach to fluorescence lifetime imaging microscopy. *Microsc Res Tech* **75**, 271–281 (2012).

5. Hinde, E. Digman, MA. Hahn, KM. Gratton, E. Millisecond spatiotemporal dynamics of fret biosensors by the pair correlation function and the phasor approach to flim. *Proc Natl Acad Sci USA* **110**, 135–140 (2013).

6. Cox, J. Neuhauser, N. Michalski, A. Scheltema, RA. Olsen, JV. and Mann, M. Andromeda: A Peptide Search Engine Integrated into the MaxQuant Environment. *J Proteome Res* **10**, 1794-1805 (2011).

7. Cox, J. and Mann, M. MaxQuant enables high peptide identification rates, individualized p.p.b.-range mass accuracies and proteome-wide protein quantification. *Nat Biotechnol* **26**, 1367-1372 (2008).